ISSN 2321-807X

Synthesis, Characterization and Application of Nano-adsorbent Materials in the Sorption of Pb(II), Ni(II), Co(II), Mn(II), Li(I) from Aqueous Solution.

H. M. H. Gad[1*], Sh. Labib[2] & M. I. Aly[3].

1-Analytical chemistry and environmental control department, Hot Laboratories and Waste Management Center, Egyptian Atomic Energy Authority, P. O. Box 13759, Inshas, Cairo, Egypt.

E-mail: hamdigad22@gmail.com.

2-Nuclear chemistry department; Hot Laboratories and Waste Management Center, Egyptian Atomic Energy Authority, P. O. Box 13759, Inshas, Cairo, Egypt.

E-mail: dr_sh_labib@yahoo.com

3-Chemistry of nuclear fuel department; Hot Laboratories and Waste Management Center, Egyptian Atomic Energy Authority, P. O. Box 13759, Inshas, Cairo, Egypt.

E-mail: mmia_2004@yahoo.com

Abstract

In this study, nano-adsorbent materials were synthesized from two different precursors by thermal activation technique. The first was the synthesizing of nano-zinc silicate from chemical reagents of zinc oxide and commercial silica gel. The second was the preparation of nano-pore size activated carbon from different biomass. The synthesized nano-adsorbent materials were characterized by different techniques; Surface Area, FTIR, XRD and SEM. The prepared nano-adsorbent materials were applied in the sorption and separation of some heavy metals from aqueous solution. These metals includes; Pb (II), Ni(II), Co(II), Mn(II) and Li(I). Some factors affecting on the sorption process (e.g. contact time and pH) were investigated. It was found that: the nano-zinc silicate (of ratio 1:1 thermally treated at 700 ^{0}C) and nano-pores activated carbon (prepared from saw dust impregnated with 70% H_3PO_4 overnight, then heated to 500 ^{0}C in presence of steam for 80 min.) were the best samples for sorption and separation of concerned heavy metals.

Key words: Nano-adsorbent; zinc silicate; activated carbons; heavy metals; sorption.

Council for Innovative Research

Peer Review Research Publishing System

Journal: Journal of Advances in Chemistry

Vol. 10, No. 8

editorjaconline@gmail.com

www.cirjac.com

ISSN 2321-807X

Introduction

Different contaminants are released to water with the rapid industrialization of human society, including heavy metal ions, organics, bacteria, viruses, and so on, which are serious harmful to human health. Among all water contaminations, heavy metal ions have high toxic and non-biodegradable properties; can cause severe health problems in animals and human beings [1, 2]. The disposal of heavy metals is a consequence of several activities like chemical manufacturing, painting and coating, mining, extractive metallurgy, nuclear and other industries [1, 2]. Therefore, the treatment and removal of heavy metal ions received considerable attention [3, 4]. Nano-materials, often possess novel size-dependent properties different from their large counterparts, many of which have been explored for applications in water and wastewater treatments [5]. In the global efforts to decrease the generated hazardous waste, green chemistry and chemical processes are integrating with contemporary developments in science and industry [6]. Hence, any synthetic route should address these principles by using friendly environmentally solvents and non-toxic chemicals [7]. A number of techniques have been developed for treating water and wastewaters embedded with heavy metals. It includes chemical precipitation, reverse osmosis, membrane filtration, solvent extraction, ion exchange and adsorption [4, 8]. Adsorption is found to be more appropriate and user friendly technique as it has a lower cost of design and operation and it is simple to apply [9, 10]. The use of nano-adsorbent materials offers significant improvement with their extremely high specific surface area, fast dissolution, high reactivity and associated sorption sites, short intra-particle diffusion distance and tunable pore size and surface chemistry [5]. For many years, silica and silica based materials have attracted great attention due to their special physicochemical properties, low cost and abundant supply and have been widely applied in many fields as molecular sieves, catalyst supports for gas absorption and separation and as raw materials for the glass industry [11, 12]. Among these materials $ZnSiO_3$ and Zn_2SiO_4 that have found widespread applications for industrial, technological and domestic purposes [11, 12]. Consequently in order to enhance the adsorptive properties of silicates it is necessary to control and adjust the morphology, specific surface area and pore size of the prepared silicates. Where, the demand for improved silica types with specific properties such as pore volume and size distribution, surface area or reactivity is fueling the search for innovative production of such materials [11, 12].

In addition to silicate, activated carbons (ACs) are the most commonly used and most effective adsorbent [10]. Nevertheless, its application fields are restricted due to its high cost [10]. The use of low-cost wastes and agriculture by-products to produce activated carbon, carbonization technique, has been shown to provide economical solution to this problem and consequently the adsorption capacities of such materials for the removal of pollutants was increased [8,10]. Especially the interest is growing in waste and wastewaters treatment using biomass based adsorbents due to their lower cost and local availability [4, 8, 9, 13-17].

The aim of this paper is to prepare nano zinc silicate and nano-pores activated carbon materials using simple routes and study the adsorption performance of the prepared nano-materials toward some selected heavy metal ions. The prepared powders will be characterized using X-ray diffraction (XRD), Fourier transform infrared spectra (FTIR), scanning electron microscopy (SEM) and specific surface area (SA) measurements. In addition some factors affecting the adsorption process such as pH, contact time and types of adsorbents and adsorbates will be investigated.

Experimental

Preparation of nano zinc silicate.

Nano zinc silicate powders were prepared using ZnO powder (99% May & baker ltd, England), SiO_2 gel powder (BDH chemicals ltd, Poole England, silica gel 60-102 mesh for chromatographic adsorption analysis) and isopropyl alcohol (99.8% Scharlau, Spain) as starting materials. All the used chemicals were of A R grade. Each powder was ground for 1hr using a mortar and pestle then sieved to 38 µm using an electrical siever (analysette siever, Germany). The sieved powders were mixed in a stoichiometric ratio (1:1) using isopropyl alcohol to make homogeneous mixtures then dried at 100 ^oC for 72 hrs and calcined at 300 ^oC for 4 hrs in an air oven at a heating rate of 10 ^oC/min. The calcined powders were sintered at 700, 800 and 900 ^oC for 3hrs in air at a heating rate of 10 ^oC/min. Table 1 shows the composition and abbreviation of the prepared samples.

Table 1: Composition and abbreviation of the prepared zinc silicate samples

Sample	Composition	Activation temperature (^oC/3 hours)	Abbreviation
SiO_2:ZnO	1:1	700	($S4_7$)
SiO_2:ZnO	1:1	800	($S4_8$)
SiO_2:ZnO	1:1	900	($S4_9$)

Where the abbreviation $S4_7$ means: S=silicate, 4=precalcined for 4 hrs before activation, 7=temperature of activation. And so on with the other samples.

Preparation of activated carbon.

The agro-residue raw material, Rice Husk (RH) and Saw Dust (SD), were supplied from El-Dakahlyia Governorate in Egypt. They were collected, washed with distilled water, dried at 110 ^oC for 48 hrs, to facilitate subsequent crushing and

grinding. The dried RH and SD were crushed and used in preparation of nano pores activated carbons by impregnation of crushed agro-residue in phosphoric acid. Starting with a 85 wt. % H_3PO_4 (BDH), the concentration of 70 % was obtained by dilution. Three equal weights of the crushed agro-residues were prepared; mixture of 50% RH and 50% SD, 100 % SD and 100% RH (samples AC_1, AC_2 & AC_3, respectively). The three samples were soaked in enough H_3PO_4 solution to cover it completely, slightly agitated to ensure the penetration of the acid throughout, then the mixture was heated to 80 ^oC for 1 hr and left overnight at room temperature to help appropriate wetting and impregnation of the precursor. The impregnated masses were dried in an air oven at 80 ^oC overnight, then, admitted into the ignition tube, which was then placed in a tubular electric furnace open from both ends. The temperature was raised at the rate of 50 ^oC/10 min, to allow free evolution of volatiles and drain of tarry matter, to attain 350 ^oC. Then the pure steam is introduced from the top of the tube using steam generator up to the hold temperatures of 500 ^oC. Soaking at final temperature was conducted for 2 hrs. The cooled masses were subjected to thorough washing with hot distilled water until the washings was neutral in effect, then dried at 110 ^oC for 48 hrs, and finally kept in tightly closed bottles.

Characterization of nano-adsorbent materials.

The prepared powders were characterized using X-ray diffraction (XRD: Shimadzu 6000 made in Japan). The used X-ray tube is a copper-tube operating at 40 KV and 30 m A and the used wavelength is $K_{\alpha 1}$ with wavelength 1.54056 Á. The scan was performed over the range 2θ (4-90) degrees. The identification of the present crystalline phases was done using Joint Committee on Powder Diffraction standards (JCPDS) database card numbers. The surface morphology of synthetic nano-adsorbent materials was examined by JEOL analytical scanning electron microscope (SEM) (JSM-6510 LA, Japan). Coarse elemental analyses were carried out from energy-dispersive X-ray spectroscopy (EDX) spectra connected to the same JOEL SEM instrument using suite version 4.05 software. The scan was performed at high vacuum mode using an accelerating voltage of 30 KV, a working distance of 20 mm and magnification X 3000. Nitrogen gas adsorption isotherms at 77K using a Quantochrome Instrument NOVA 1000e (USA) was used to determine the surface area, total pore volume and average pore size of the nano-adsorbent materials. At the beginning the sample was degassed at 300 °C for >3 hrs to drive off moisture and any other volatile material that could interfere with the adsorption of nitrogen. Surface area of the samples was calculated from Brunauer-Emmett-Teller (BET) equation. Fourier transform infrared (FTIR) spectra of nano-adsorbent materials were recorded on Pomen, Hartman Spectrophotometer with KBr pellet technique in the mid-infrared range (4000 to 400 cm^{-1}) with 4 cm^{-1} resolution.

Application of the prepared nano-adsorbents in the sorption of some heavy metals.

The synthesized nano-zinc silicate and nanopores-activate carbons were used in the sorption of Pb(II), Ni(II), Co(II), Mn(II), Li(I) from aqueous solution to investigate the adsorption capacity of these new materials in addition to the reclamation of these valuable metal for reuse in industrial purposes. To achieve that, some factors were investigated: type of adsorbent and adsorbate, contact time and pH.

Batch adsorption studies.

To study the effect of contact time, pH of solution, type of adsorbent and adsorbate; the sorption experiments of heavy metal on synthetic nano adsorbents were carried out at constant temperature (25 ± 1 ^oC) using 50 mL polypropylene tube with screw cap. The solutions pH was adjusted by additions of HNO_3 or NaOH and the pH values at the beginning and the end of experiments were measured using a digital pH meter of Hanna Instruments type at the ambient laboratory temperature degree 25 ± 1 ºC with a BNC waterproof electrode. All tests were conducted using 0.05 gm of adsorbent with 10 ml solutions containing the metal ions of initial concentration 50 mg/l for various time ranged from 5 to 120 minutes. In all cases, the sorbents were removed from the solutions by centrifugation for 20 min at 4000 rpm using Hettich Centrifuge, model ROTOFIX 32 A. Atomic Absorption Spectrometer (AAS), Model (S4) thermo Electron Corporation was used for the measurement of the metal ions concentration in the aqueous phase. For batch investigation, a good shaking for the two phases was achieved using a thermostatic mechanical shaker of the type Julabo SW-20 C, Germany. The amount of metal adsorbed was calculated by the simple mass balance relationship:

$$Q_e=(C_o-C_e) \times V/W \qquad (1)$$

Where C_o and C_e are initial and final concentration, V is the volume of solution per liter and W is the weight of adsorbent in gm. And the % removal of each metal was calculated from the following equation:

$$\% \text{ removal} = (C_o-C_e)/C_o \times 100 \qquad (2)$$

Results and discussion

The adsorption of contaminants depends on many factors among them, the properties of the adsorbents (i.e. particle size, porous structure, surface chemistry) [18]. Accordingly, an effort was done to produce nano-materials with a better properties and performance than used before using a simplified materials and methods. Usually, the fabrication of Zn_2SiO_4 ceramics could be achieved by solid-state sintering process at a sintering temperature of 1300 ^oC [19]. It was found that Zn_2SiO_4 could be formed at a lower sintering temperature ~ 900 ^oC by the addition of the pre-treated $BaO-B_2O_3$ or $H_2SiO_3-H_3BO_3$ mixtures, which had the potential to transform into a melt at relatively low sintering temperature (869-900) ^oC, to the pre-sintered mixed $ZnO-SiO_2$ [19]. In our study, we tried to synthesize nano Zn_2SiO_4 at a lower temperature, < 900 ^oC, than used previously by using a simple conventional solid-state applying “hard ground and sieving” technique for the used precursors. Therefore this pretreatment allowed the use of precursors having small particle sizes which could penetrate into the nano-regime and became active to make solid state interaction between the precursors at a

lower sintering temperature. Also our target was not only to prepare Zn_2SiO_4, as a pure phase, but also we wanted the presence of $ZnSiO_3$ as a secondary phase to benefit from its presence in increasing the adsorption efficiency of the used nano-materials. Concerning the ACs, the literatures showed several studies related to the conversion of lignocellulosic materials into activated carbons (ACs) describing the large varieties of activation processes existing (physical and chemical activations) with emphasis on their advantages and drawbacks as well as the adsorption capacity development and the changes on the surface chemistry as a function of the experimental variable used [20]. The material was physically activated by carbonization under inert atmosphere then activated at high temperature using either steam or carbon dioxide as the activating reagent [21]. Otherwise in the chemical activation, the precursor was treated with chemical to help with initial dehydration [21]. In most cases, the chemical activation was preferred over physical activation due to the fact that it was commonly used for biomass precursor for achieving higher yields and larger surface areas [21]. The prepared ACs have been activated with phosphoric acid, where several studies in the literature have been concerned with H_3PO_4 activation of lignocellulosic precursors to ACs with well-developed pore structures in higher yields at relatively lower temperatures than physical activations [22].

Characterization of synthesized nano-adsorbent materials.

X-Ray Diffraction Analysis (XRD).

Figure 1(a-c) shows the X-ray diffraction pattern of the prepared nano zinc silicate powders thermally activated at 700, 800 and 900 ^oC for 3hrs, respectively. $S4_7$ was characterized by the presence of both Zn_2SiO_4 having rhombohedral structure with space group R $\bar{3}$(148) (JCPDS 70-1235) as a major phase and $ZnSiO_3$ having orthorhombic structure with space group Pbca (61) (JCPDS 70-0852) as a minor phase as shown in Figure 1 (a). No peaks for ZnO or SiO_2 were observed indicating the complete solid state reaction between the reactants leading to the formation of $ZnSiO_3$ and Zn_2SiO_4. The broadening of the diffraction peaks suggested that the particle size of the two phases was very small. The average particle size (D) is 57.5 nm for Zn_2SiO_4 and 58.7 nm for $ZnSiO_3$ as given from the Debye- Scherrer equation [23]:

$$D = 0.94\lambda / \beta \cos\Theta \qquad (3)$$

Where; **λ** is the wavelength of the X-ray radiation used and β is the full width at half intensity maximum (FWHM) in radian. No change in the structural behavior of $S4_8$ and $S4_9$ was observed, Figure 1(b-c). An increase of the obtained diffraction peaks sharpness was observed in $S4_8$ due to the particle size growth of Zn_2SiO_4 and $ZnSiO_3$ to 68.5 nm and 70.7 nm respectively, Figure 1 (b). Otherwise a decrease in the grain size of Zn_2SiO_4 to 65 nm and slight increase in grain size of $ZnSiO_3$ to 71.3 nm was observed in $S4_9$, Figure 1 c.

ISSN 2321-807X

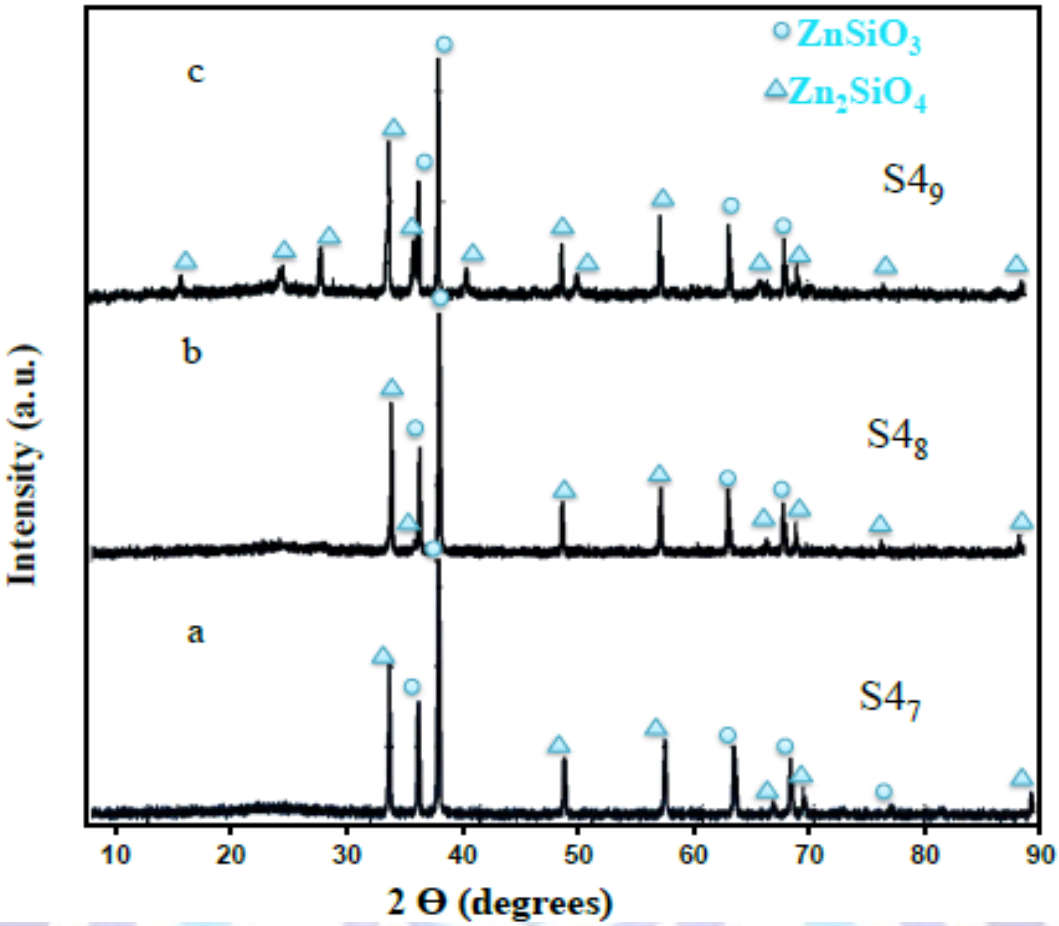

Figure 1: XRD of the prepared nano zinc silicate powders thermally treated at 700, 800 and 900 ^{o}C for 3h.

XRD revealed that both of $ZnSiO_3$ and Zn_2SiO_4 were synthesized at annealing temperatures of 800 and 900 ^{o}C with onset growth at 700 ^{o}C. Moreover, the XRD results showed that the composition of the Zn_2SiO_4 powders annealed at 800 and 900 ^{o}C consisted of higher concentration of crystalline Zn_2SiO_4 as the temperature increased. This emphasized that the synthesis of Zn_2SiO_4 was achieved at 900 ^{o}C. This was lower than the reported temperature for solid-state reaction to produce zinc silicate [24, 25]. Thus, increasing the annealing temperature and soaking time may induce the complete conversion of the unreacted zinc oxide and silicon dioxide. However, the possibility of producing a different compound was plausible and need to be explored further [24].

Scanning Electron Microscopy (SEM-EDX).

Scanning electron microscopy (SEM) of the prepared activated carbons, Figure 2, showed that the texture and developed porosity was strongly affected by characteristics of the starting materials. AC that has the highest surface area as will be shown latter, was obtained from SD. Elemental analysis of the activated carbon was accomplished using energy dispersive X-ray spectroscopy (EDX).

ISSN 2321-807X

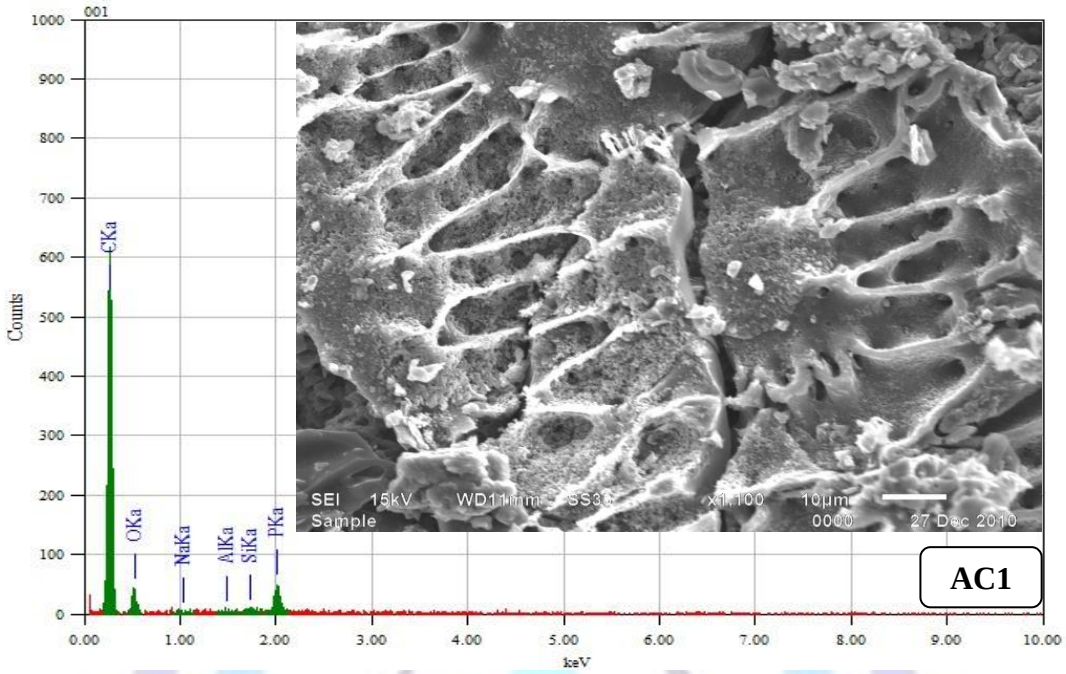

AC_1 (50% RH + 50% SD)

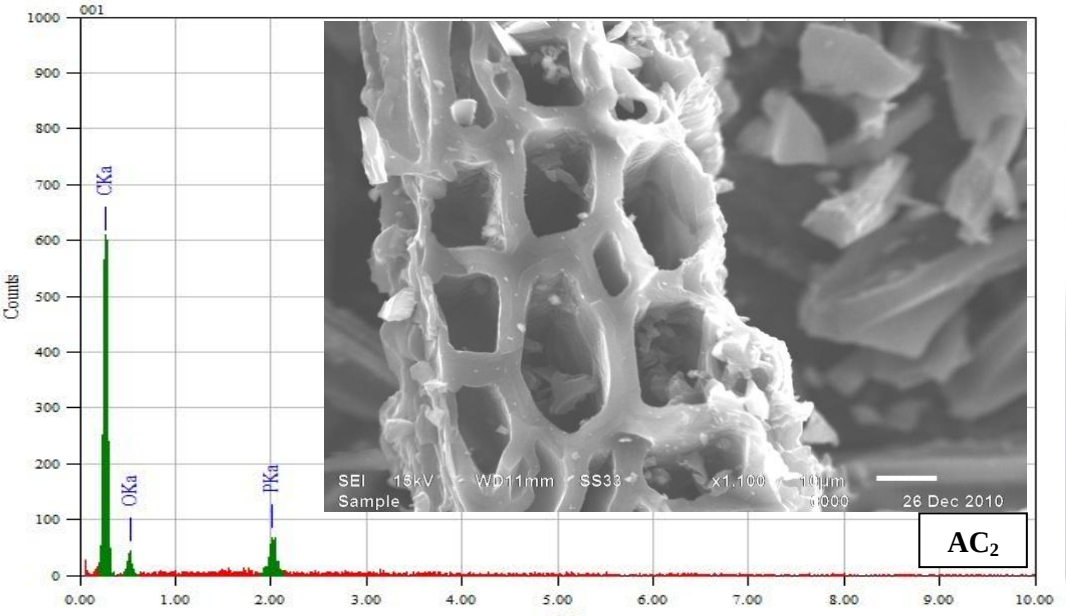

AC_2 (100 % SD)

ISSN 2321-807X

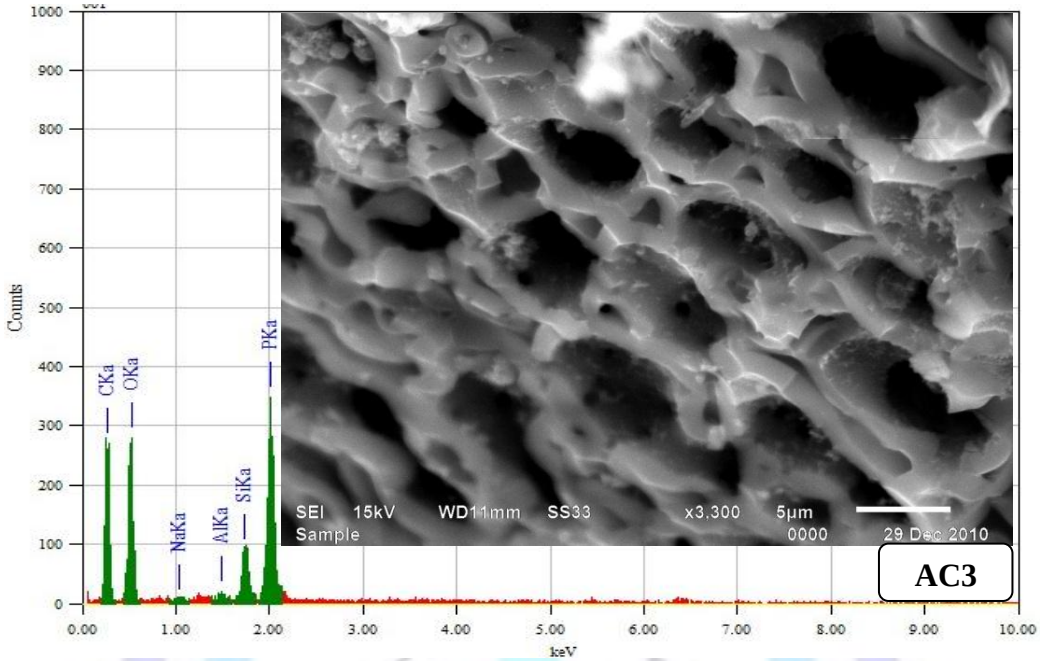

AC_3 (100 % RH)

Figure 2: Scanning electron microscopy (SEM) and EDX of prepared activated carbons.

EDX analysis revealed that the AC_1 sample contained P, Si, Al, Na, O and C where the AC_2 sample contains P, O and C only. The presence of P comes from the H_3PO_4 used in the activation process; O and C came from the cellulosic material of the two precursors, but the presence of Si, Na and Al in the AC_1 came from RH precursor. Therefore, these elements were present with considerable amount in AC_3 sample which is only RH. According to Galiatsatou et. al. [26], the pores of activated carbons was classified into three groups depending on the pore width (pw): microspores (pw < 20Å); transitional mesopores (20 Å < pw < 500 Å); macro pores (pw > 500 Å). During adsorption, macro and mesopores allowed rapid transport of the adsorbate into the interior of carbon for subsequent diffusion into micropore volume. Consequently, a well-developed porous network in all pore size ranges results in improved adsorption properties of the carbon.

Fourier transforms infrared (FTIR) spectra.

The prepared zinc silicate powders thermally treated at 700, 800 and 900 ^oC were further characterized using FTIR, Figure 3. The FTIR spectra showed dominant peaks between 488 to 3495 cm^{-1}. Where, the spectral region at 1100 cm^{-1} was characterizing for the asymmetric Si-O stretching [27]. All samples showed this strong band (~ 1100 cm^{-1}) with slight shift due to the variation in particle size values of the different samples with the temperature as given from XRD. Bands at 897.9, 1097.8, 2335.8 and 2361.1 cm^{-1} were attributed to SiO_4 asymmetric stretching vibration modes [28]. Bands at 933-940 cm^{-1} were attributed to Si-O-Zn stretching of both $ZnSiO_3$ and Zn_2SiO_4 phases.

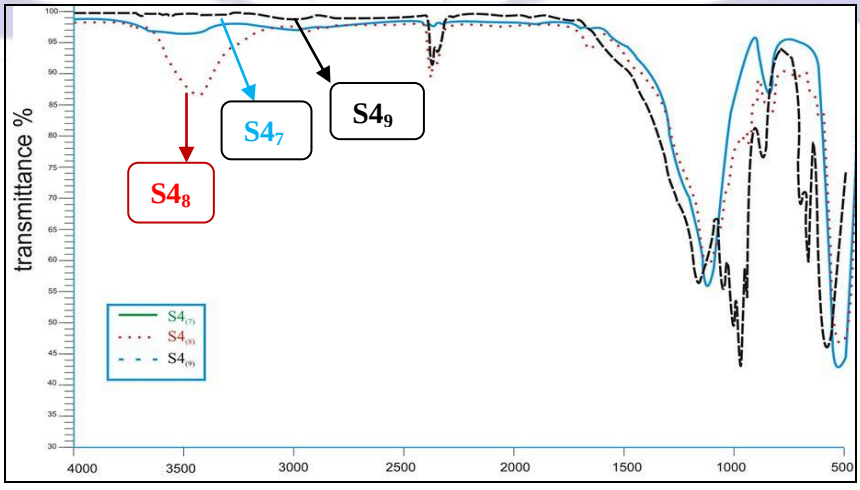

Wave number (cm^{-1})

Figure3: FTIR of the prepared nano zinc silicate powder thermally treated at 700, 800 and 900 ^oC for 3h.

ISSN 2321-807X

On the other hand the lower bands at 480-500 cm^{-1} were characteristic for ZnO_4. Also, bands at 600-610 cm^{-1} specified the growth of Zn_2SiO_4 at this temperature [28]. Beside the given asymmetric stretching vibrations outlined above, the FTIR spectra of the synthesized powders annealed at 800 and 900^oC exhibited symmetric stretching and deformation vibration modes of ZnO_4 and SiO_4 as observed in Figure 3. Based on previous studies of Zn_2SiO_4 synthesized using solid-state reaction, annealing temperature must be between 1100 and 1400^oC to produce zinc silicate [25]. However, FTIR spectra of the synthesized zinc silicate powders annealed at 700^oC showed the vibrations corresponding to ZnO_4 and SiO_4 groups indicating the growth of Zn_2SiO_4, as shown in Figure 3.

Thus, FTIR spectra of zinc silicate powders annealed at 800 and 900^oC have shown all wave numbers pointing to ZnO_4 and SiO_4 of Zn_2SiO_4 and $ZnSiO_3$ indicating that Zn_2SiO_4 powders were produced at these temperatures.

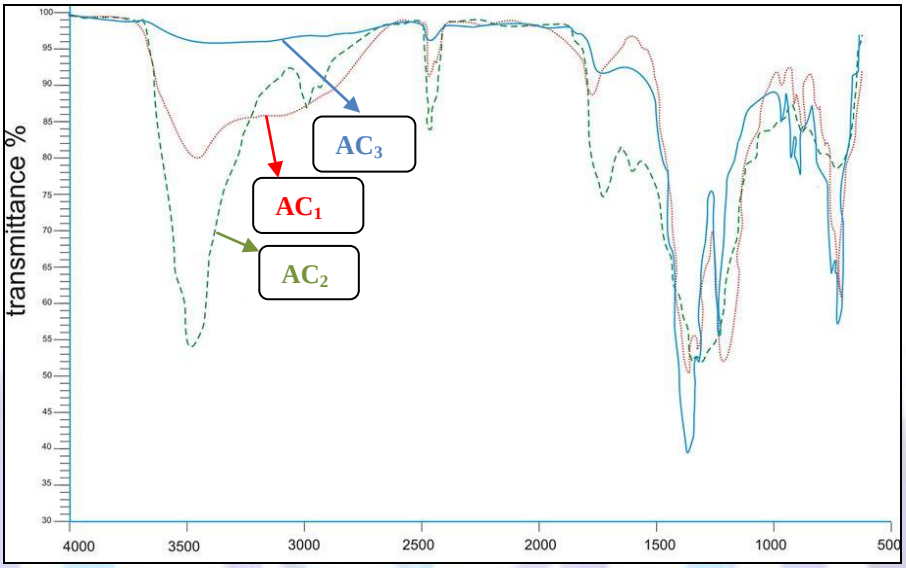

Fig. 4: FTIR of the prepared activated carbon from different precursors.

With respect to the prepared activated carbon, the spectra shown in Fig. 4 shows the FTIR of three prepared samples; AC_1, AC_2 and AC_3 which prepared from precursor as mentioned above. The FTIR of AC_1 displayed a number of absorption peaks, indicating the complex nature of the surfaces of this sample as it contained peaks presented in the other two samples as it prepared from 50% RH and 50% sawdust. The broad peak at 3418.6 cm^{-1} can be attributed to the hydrogen-bonded OH group of alcohols and phenols [29]. This peak shifted to sharp one at 3428.4 cm^{-1} in the AC_2 prepared from SD only and it shifted to 3391.8 cm^{-1} in the AC_3 prepared from RH only. Also, these bands could be arising from the N-H stretching vibration in primary amines. The band at 2917.7 cm^{-1} in AC_2, arises from the –CH stretch of a methylene [30].

Also, the peak at 1189.3 cm^{-1} in $AC_1$was associated with C-O stretching vibrations in carboxylic acids [31], this peak shifted to 1161.6 cm^{-1} in AC_2 and it shifted to 1185.5 cm^{-1} in AC_3 (prepared from RH+SD) confirming the peak present in AC_1(prepared from RH only). These major shifts in band suggested that the alcohols/phenols and carboxylic acid groups were involved in metal binding. In addition, the band at 1597.0 cm^{-1} represents the C=C skeletal stretch in condensed aromatic system and a peak at 754.2 cm^{-1} could be assigned to the out-of-plane C-H bending modes of an aromatic compound [32]. Agricultural biomasses mainly consist of lignin, cellulose, hemicelluloses and some proteins which made them effective adsorbents for dissolved solids.

Surface Area Analysis

Nitrogen adsorption, because the relatively small molecule diameter of nitrogen, is frequently used at 77 K to determine porosity and surface area and to be a standard procedure for the characterization of porosity texture of carbonaceous adsorbents.

The adsorption isotherm is the information source about the porous structure of the adsorbent, heat of adsorption, characteristic of physical and chemical adsorption and so on. Adsorption isotherm may be grouped to six types. Prepared adsorbents exhibited adsorption isotherm of type IV according to IUPAC [33]. The type IV isotherm represents the micro–mesoporous structure of the adsorbents. The initial part of the isotherm follows the same path as the corresponding type II isotherm and therefore the result of monolayer–multilayer adsorption on the mesopore walls [34]. The type (IV) isotherms with H_1- type Hysteresis loop, described the presence of tubular capillaries pores in between the particles [35, 36]. The

ISSN 2321-807X

BET surface area (S_{BET}), Langmuir surface area, total pore volume and average pore radius results obtained by applying the BET equation to N_2 adsorption at 77 K are listed in Table 1. As seen from this table, the pore diameters of the prepared samples were in the range of nano-porous diameters.

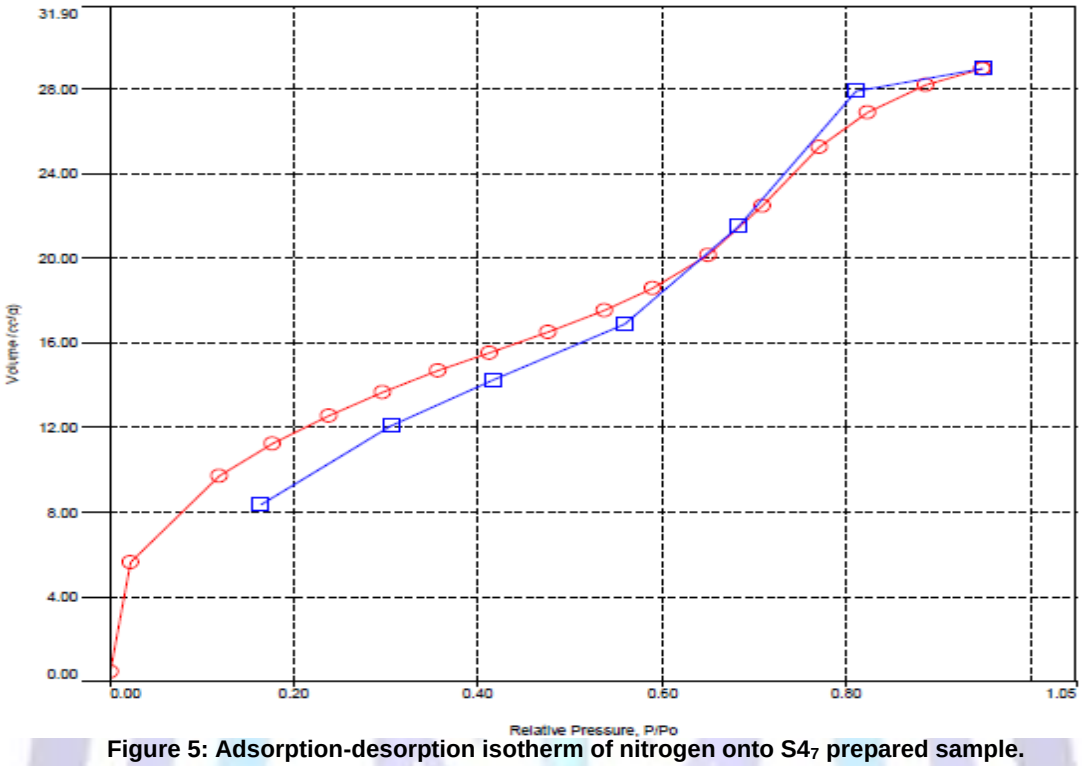

Figure 5: Adsorption-desorption isotherm of nitrogen onto $S4_7$ prepared sample.

Table 2: Surface area analysis of the prepared adsorbents.

Parameters	$S4_7$	$S4_8$	$S4_9$	AC_1	AC_2	AC_3
BET Surface area (m^2/g)	44.14	36.06	33.09	17.96	1109.98	324.12
Langumir surface area	68.24	56.65	0.00	30.25	1598.25	487.36
Total Pore volume (cc/g)	$4.476\ e^{-02}$	$2.798e^{-02}$	$1.808\ e^{-03}$	$1.829e^{-02}$	$7.27e^{-01}$	$2.379e^{-01}$
Average pore radius (Å)	$2.028\ e^{+01}$	$1.92616e^{+01}$	$1.093e^{+00}$	$2.037e^{+01}$	$1.31e^{+01}$	$1.468e^{+01}$
Pore diameter (nm)	4.056	3.852	0.218	4.074	2.62	2.936

As seen from table (2): with respect to zinc silicate sample, as the temperature of preparation increases the surface area, total pore volume and pore diameter decreases. This may be due to the increase of the formation of crystalline form of silica. While in the case of activated carbon samples, these parameters seem to be dependant mainly on the type of precursors of the activated carbon.

Application on the synthetic nano-adsorbents in the sorption of heavy metals.

Most of heavy metal ions are toxic to living organisms. These metal ions are non-degradable and are persistent in the environment. Therefore, the elimination of heavy metal ions from wastewater is important to protect public health. Sorption is considered as a very effective and economical process for metal ion removal from wastewaters. There are many factors affecting on the adsorbent materials in the sorption of metal ions present in aqueous solutions. In the following we will investigate some of these factors.

Sorption depending on the type of adsorbent.

The different prepared nano-adsorbents materials were applied to study its efficiency in adsorption and separation of Pb(II), Ni(II), Co(II), Mn(II) and Li(I) and the results were listed in table 3. As seen from this table:

ISSN 2321-807X

Table 3: Effect of adsorbent type on % removal of studied heavy metals.

Nomenclature	% Removal of the studied heavy metals					**Total capacity**	Difference between ZS & AC
	Pb(II)	Ni(II)	Co(II)	Mn(II)	Li(I)		
Electronegativity	1.87	1.91	1.88	1.55	0.98		
$S4_7$	100	12.5	99.8	36.8	--	**249.1**	723.0
$S4_8$	100	15.0	99.9	28.1	--	**243.0**	
$S4_9$	99.8	15.0	99.9	12.8	3.4	**230.9**	
AC_1	99.8	--	99.7	29.8	4.1	**233.4**	749.6
AC_2	100	10.0	94.4	--	3.8	**208.2**	
AC_3	98.0	5.00	100	100	5.0	**308.0**	
Total % R	**597.6**	**57.0**	**593.7**	**207.5**	**16.3**		

(1) The total capacity of the zinc silicate samples decreased as the temperature of preparation increased. This may be due to the decrease of the surface area and total pore volumes.

(2) The total capacity of the prepared activated carbon did not depend on the surface area but depends on the type of the precursor and the sample prepared from rice husk only was found to have the highest adsorption capacity and this may be due to the high content of silanol groups in this sample giving the chance of exchange of metal ions with hydrogen ions of these groups.

(3) If we have a binary mixture of metal ion of Li(I) and one of other metals, the prepared zinc silicate (ZS) samples can be used to separate Li(I) from the second metal ion in the same solution. This may be due to the higher electronegativity of later ions than that of Li(I) ion.

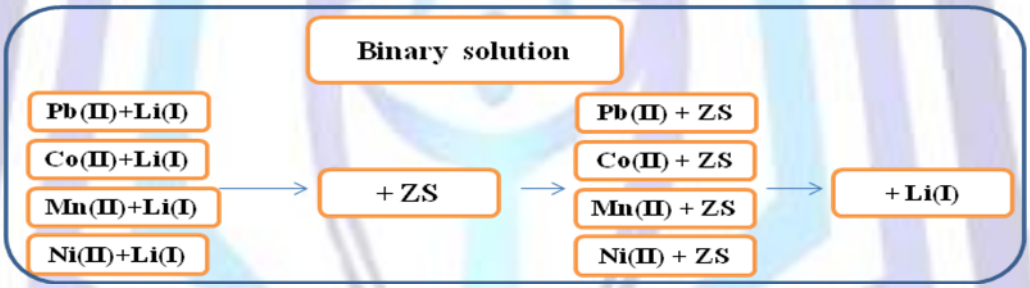

Fig 6: Separation of studied heavy metals using prepared nano-zinc silicate (ZS).

(4) The same behavior was observed with the ACs samples but with different details. The highest % removal was obtained by AC_3 which was prepared from rice husk only and the lowest value obtained by AC_2 which was prepared from sawdust only.

(5) The total capacity of % removal of prepared AC is higher than that of ZS samples.

As indicated from Table 2, $S4_7$, $S4_8$ and AC_1, AC_2 could be used as good adsorbents for the adsorption and separation of binary mixtures of metal ions. Irrespective of the type of the adsorbed metal ions, the efficiency of the studied adsorbents was related to their microstructures, surface structures and pore size distribution. $S4_7$ was characterized by a tailored nanostructure as given in the XRD. Which in turn could be beneficial in providing an increased surface area that aid to the transport of metal ions from the liquid phase to the reaction sites of $S4_7$ [37]. Meaning that the nanostructure played an important role in enhancing the chance of decreasing the energy of adsorption of metal ions and decreasing the diffusion path barrier at liquid-solid interface. Beside AC_2 was characterized by a higher specific surface area when compared to the other prepared ACs, its structure was characterized by a regular tubular developed pores having smooth surface as shown in the SEM. In this case a regular network of interconnected pore channels could facilitate ion transport by providing smaller resistance and shorter diffusion pathway [32].

Effect of heavy metal ions

There is no consensus in the competitive adsorption of metal ions, as researchers have attributed their different affinities to different factors [38]. These factors were related to the properties of these ions in aqueous solution and could affect surface binding and interaction energies or the accessibility of surface centers which could be linked to the size of the species adsorbed [38]. The transportation of the adsorbate ions from the solution phase to the surface of the adsorbent particles was controlled by mass transfer diffusion, pore diffusion, surface diffusion, and adsorption into the interior surface of the adsorbents or a combination of one or more steps [14]. Consequently the maximum adsorption

amount of the tested heavy metals on the used adsorbents depends on the adsorption mechanism [39]. Many papers translate the high percentage of the adsorption of Pb(II) onto the used adsorbents to its high electro-negativity [21]. Consequently the order of affinity to the adsorbate must be: Ni(II) > Co(II) > Pb(II) > Mn(II) > Li(I), which didn't fit with the obtained results, as given in table (2). So we couldn't classify the order of metal ions removal on the basis of electronegativity. Sometimes the adsorption of metal ions was associated to the size of the ions and the pore development, i.e. the smaller the size of the metal ions the easier its adsorption [40- 41] meaning that Pb (II) having ionic radius (1.19 A^o) must be less adsorbed than the Li (I) (0.076 A^o), Mn (II) (0.070 A^o), Co (II) (1.25 A^o) and Ni (II) (0.070 A^o), this trend didn't also match with the obtained results where: the adsorption order is Pb(II) > Co(II) > Mn(II) > Ni(II) > Li(I) as seen from table (2). The reason of the high percent removal of metals having large ionic size may be explained in term of hydration energy: where in the large non hydrated ions, the charge was more dispersed and the hydration energy was held less strongly [32]. So the bigger the ionic radius, the stronger the adsorption of the ion since the hydration capacity of that ion was smaller resulting in weaker binding of the ion and water phase [32].

Effect of contact time.

The time needed for the interaction between the adsorbate and adsorbent is crucial: (the faster the removal, the better the adsorbent). Hence, it is important to study the effect of contact time on the removal of the selected heavy metal ions [38]. The effect of contact time on the efficiency of $S4_7$ and AC_2 for the adsorption of concerned heavy metal ions was investigated, Figure 7. Where, the initial concentration of the selected heavy metal ions was kept constant (50 mg/L).

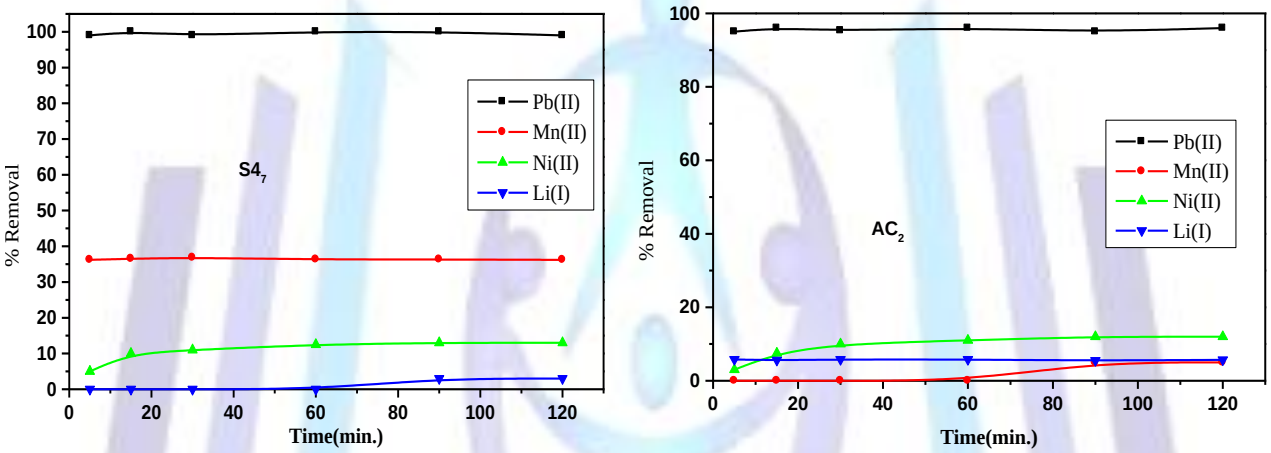

Figure 7: % Removal of Zn-silicate ($S4_7$) and activated carbon (AC_2) for different metal ions.

The heavy metal percent adsorption increased with contact time until the equilibrium was attained. According to the given data, it was found that 30 min was sufficient for two adsorbents to reach the equilibrium and became saturated with the studied metal ions as shown from the given plots. The studies conducted on the adsorption of Pb^{+2} removals revealed that (95-99) % of this metal ion was removed within the first 5 min from $S4_7$ and AC_2, respectively. The fast adsorption at the initial stage was probably due to the increased concentration gradient between the adsorbate in the solution and the adsorbate in adsorbent [42]. Where, there must be an increased number of vacant sites available at the beginning [42], As the surface adsorption sites became exhausted, the uptake rate was controlled by the rate at which the adsorbate was transported from the exterior to the interior sites of the adsorbent particles [43]. So the initial fast uptake was done through a physical adsorption since adsorption tends to attain in instantaneous equilibrium. But there was another important factor that influence the adsorption process was the characteristics of the adsorbent's surfaces [18]. As the contact time was increased, more and more functional groups participated in adsorption of the metal ions [42].

Effect of pH

The pH of the solution has a great influence on the adsorption capacity of a porous material. The acidity of the solution affects previously this capacity, because the superficial charge of the adsorbent is a function of the solution's pH [21]. In aqueous solutions the cationic species depend on the pH of the solution and the total concentration of metal ions [21]. At a certain pH range, most metal adsorption increases with increasing pH up to a certain pH value and then decreases with further increasing pH [15]. Therefore, there is a favorable pH range for the adsorption of every metal on a specific adsorbent [15]. Where, these ions exist as ions until the pH of solution at 6.0 [21].

At low pH (< 3), the prepared adsorbent surface could have a positive charge, so the electrostatic repulsion takes place between the same charge of the cations and the adsorbent surface [21]. The adsorption of the selected heavy metal ions could be influenced by the existence of the chemical surface groups and the pH of the solution [21]. Porous materials possessing a large surface area could possess high adsorption capacities toward the heavy metals [39]. Functional groups such as carboxyl, amine and hydroxyl on the surface could provide complexation with the heavy metal ions [39]. Functional groups containing oxygen or nitrogen atoms could provide nonbonding electrons to coordinate with the divalent metals [39]. Consequently, complexation became a key factor in determining the adsorption capacities [39].

ISSN 2321-807X

In this study, the effect of pH on the selected heavy metals ions by $S4_7$ and AC_2 was investigated at different pH (0.5, 3 and 4) and shaking the suspensions for varying contact times (5-120 min), table 4. For $S4_7$, irrespective of the studied contact times, the percent of the adsorption of the studied heavy metals ions significantly increased at pH 3 then was kept constant at pH 4 for Pb (II), Ni (II), increased for Li (I) and decreased for Mn (II). In general, it was known that at low pH (< 3), there was excessive protonation of the active sites at the adsorbent surface squeezing out the already adsorbed metal ions [4, 43]. At moderate pH values (3-6), linked H^+ was released from the active sites and the adsorbed amount of metal ions was found to increase [4, 43]. It could be observed that the uptake was highly dependent on the solution pH, where a marked increase in the adsorption capacity of Pb^{+2} and Ni^{+2} ions from pH 0.5 to 3 was observed, as shown in table (3). This observation may be due to the differences in the degree of surface protonation of the prepared zinc silicate's and activated carbon surface with varying the pH [44]. With respect to $S4_7$, based on the assumed incongruent dissolution of zinc silicate, the dominant equilibrium for the zinc silicate over a wide range of pH is:

$$Zn_2SiO_4 + 2H_2O \rightleftharpoons 2ZnO + Si(OH)_4 \qquad (4)$$

Accordingly, the surface activity could be translated to a reactive silanol group (-Si-OH) [45]. The major mechanism of adsorption of cations was ion-exchange with the replacement of hydrogen ions of the surface of silanol groups with the present metal ions, especially at low pH [46, 47]. The sorption of metal ions on $S4_7$ was mainly a two-step processs: fast adsorption of metal ions on the external surface by ion-exchange between the hydrogen ion of silanol group with the present metal ions followed by the intra-particle diffusion along the pore walls [32]. Their nanoscale counterpart had high adsorption capacity and faster kinetics because of the higher specific surface area, shorter intra-particle diffusion distance as outlined before and larger number of surface sites (i.e. corners, edges, vacancies) [5, 26].

For AC_2, the effect of pH may be explained in the terms of pH_{zpc} (zero point of charge) of the adsorbent, at which the adsorbent was neutral. The surface charge of the adsorbent is positive when the suspension pH was below pH_{zpc}. Moreover, at pH lower than pH_{zpc}, the predominant metal species will be positively charged [M^{n+} or $M(OH)^{(n-1)+}$]. Thus, the uptake of metals in the pH range below the pH_{zpc} is a H^+ M^{n+} or $(M(OH)^{(n-1)+})$ exchange process [15]. An increase in the adsorption as long as the metal species were still positively charged or neutral event though the surface of the adsorbent was negatively charged [14, 15]. When both the surface charge of the adsorbent and the metal species charge become negative, the adsorption will decrease significantly. Oxygen was an important heteroatom that commonly occured in ACs in the form of carboxylic groups which enhanced the acidity of the ACs surface [18] and increased the adsorption of metal ions at the external surface through ion exchange process.

Table 4: Effect of pH on the % removal of studied heavy metals using $S4_7$ and AC_2.

pH	Time (min.)	% Removal							
		Pb(II)		Ni(II)		Mn(II)		Li(I)	
		$S4_7$	AC_2	$S4_7$	AC_2	$S4_7$	AC_2	$S4_7$	AC_2
pH=0.5	5	60	50	2	0	15	0	0	2.1
	15	65	66	3	5	20	0	0	2.2
	30	68	63	5	5.5	25	0	0	2.3
	60	70	66	7	7	27	0	0	3.0
	90	72	70	9	11	30	0	0	5.0
	120	72	70	9	11	30	0	0	5.0
pH=3	5	98	96	7	5	15	0	0	6.0
	15	98	96	15	9	20	0	0	6.5
	30	99	98	15	12	25	0	0	7.0
	60	99	97	20	15	28	0	0	7.0
	90	100	97	25	15	27	0	3	7.1
	120	100	97	25	15	28	0	3	7.0
pH=4	5	98	90	7	5	14	0	0	7
	15	99	94	15	11	18	0	0	7
	30	99	95	17	15	22	0	0	7
	60	98	95	24	17	26	0	0	10
	90	99	96	25	17	27	0	0	10
	120	99	96	25	18	26	0	0	10

As shown in the results, the increase in pH from 0.5 to 3 showed an increase in the amount of the adsorption of Pb (II), Ni (II) and Li (I) and a marked decrease in the amount of the adsorption of Mn (II). Further increase in the pH to 4 showed a decrease in the amount of the adsorbed Pb (II) and Mn (II). The increase in the amount of the adsorbed metal ions with increasing the pH from 0.5 to 3 may be explained to the deprotonation of the different active sites present on the AC_2, as explained before, giving the chance of the linking of the selected metal ions on these sites. Otherwise the decrease of the adsorption of Mn (II) with increasing the pH may be explained to the presence of Mn (II) in hydrated form. Consequently, Mn^{+2} ions preferred to be in solution than to be adsorbed [19].

Conclusion

From this study we can concluded that:

- XRD reveals that: a) both of $ZnSiO_3$ and Zn_2SiO_4 were synthesized at annealing temperatures of 800 and 900 ^oC with onset growth at 700 ^oC. b) The composition of the Zn_2SiO_4 powders annealed at 800 and 900^oC consisted of higher concentration of crystalline Zn_2SiO_4 as the temperature increased.
- Scanning electron microscopy (SEM) of prepared activated carbons showed that the texture and developed porosity was strongly affected by characteristics of the starting materials. AC that has the highest surface area was obtained from Saw Dust.
- The BET surface area revealed that: with respect to zinc silicate sample, as the temperature of preparation increased the surface area, total pore volume and pore diameter decreased. While in case of activated carbon samples, these parameters seem to be dependant mainly on the type of precursors of the activated carbon.
- In the application of the prepared nano-adsorbent materials in the sorption and separation of studied heavy metals it was found that: (i) the total capacity of the zinc silicate samples decreased as the temperature of preparation increased. (ii) The total capacity of the prepared activated carbon did not depend on the surface area but depends on the type of the precursor and the sample prepared from rice husk only was found to have the highest adsorption capacity. (iii) The total capacity of prepared ACs is higher than that of ZS samples. (iv) If we had a binary mixture of metal ion of Li (I) and one of other metals, the prepared zinc silicate (ZS) samples could be used to separate Li (I) from the second metal ion in the same solution.
- From the factors affecting the removal of studied heavy metal, it was found that: (1) the adsorption order is Pb(II) > Co(II) > Mn (II) > Ni(II) > Li(I), (2) it was found that 30 min was sufficient for $S4_7$ and AC_2 adsorbents to reach the equilibrium, (3) the increase in pH from 0.5 to 3 showed an increase in the amount of the adsorption of Pb (II), Ni (II) and Li (I) and a marked decrease in the amount of the adsorption of Mn (II).
- Therefore, from the characterization and application of the prepared nano-adsorbent materials, it could be used in sorption and separation of some heavy metals as shown in our study.

References

[1] Wang X., Guo Y., Yang L., Han M., Zhao J. and Cheng X., Nanomaterials as Sorbents to Remove Heavy Metal Ions in Wastewater Treatment. J.Environ. and Anal.Toxicology,2 7 (2012), 1-7.

[2] Quintelas C., Rocha Z., Silva B., Fonseca B., Figueiredo H., Tavares T., Removal of Cd(II), Cr(VI), Fe(III) and Ni(II) from aqueous solutions by an E. coli biofilm supported on kaolin. Chem. Eng. J. 149 (2009) 319–324.

[3] Pagana A. E., Sklari S. D., Kikkinides E. S., Zaspalis V. T., Microporous ceramic membrane technology for the removal of arsenic and chromium ions from contaminated water. Microporous Mesoporous Mater. 110 1 (2008), 150-156.

[4] Bo˘zic D., Stankovi´c V., Gorgievskia M., Bogdanovic G. and Kovacevic R., Adsorption of heavy metal ions by sawdust of deciduous trees. J. Hazard. Mater. 171 (2009) 684–692.

[5] Qu X., Alvarez P. J.J. and Li Q., Applications of nanotechnology in water and wastewater treatment. Water Res. 47 (2013), 3931-3946.

[6] De Simone J. M., Practical Approaches to Green Solvents. Science. 297 5582 (2002), 799-803.

[7] Raveendran P., Fu J., Wallen S.L., Completely green synthesis and stabilization of metal nanoparticles. J. Am.Chem. Soc. 125 (2003), 13940-13941.

[8] Sreejalekshmi K. G., Krishnan K. A. and Anirudhan T. S., Adsorption of Pb(II) and Pb(II)-citric acid on sawdust activated carbon: Kinetic and equilibrium isotherm studies. J. Hazard. Mater. 161 (2009), 1506–1513.

[9] Yadav A. K., Abbassi R., Gupta A. and Dadashzadeh M., Removal of fluoride from aqueous solution and groundwater by wheat straw, sawdust and activated bagasse carbon of sugarcane. Ecol. Engineering 52 (2013), 211– 218.

[10] Baccar R., Bouzid J., Feki M. and Montiel A., Preparation of activated carbon from Tunisian olive-waste cakes and its application for adsorption of heavy metal ions. J. Hazard. Mater. 162 (2009), 1522–1529.

[11] Lu Q. and Yun G., Facile one-step solid-state reaction route to synthesize ordered mesoporous ß-Zn_2SiO_4–SiO_2 nanocomposites. Ceram Int. 39 (2013), 3533–3538.

[12] Laurentowska A. and Jesionowski T., Physicochemical Problems of Mineral Processing 48 1 (2012), 63-76.

[13] Noonpui S., Thiravetyan P., Nakbanpote W. and Netpradit S., Color removal from water-based ink wastewater by bagasse fly ash, sawdust fly ash and activated carbon. Chem. Eng. J. 162 (2010), 503–508.

[14] Foo K.Y. and Hameed B. H., Mesoporous activated carbon from wood sawdust by K_2CO_3 activation using microwave heating. Bioresour. Technol. 111 (2012), 425–432.

[15] Semerjian L., Equilibrium and kinetics of cadmium adsorption from aqueous solutions using untreated Pinus halepensis sawdust. J. Hazard. Mater. 173 (2010), 236–242.

[16] Nanseu-Njiki Ch. P., Dedzo G. K. and Ngameni E., Study of the removal of paraquat from aqueous solution by biosorption onto Ayous (Triplochiton schleroxylon) sawdust., J. Hazard. Mater. 179 (2010), 63–71.

[17] Asadi F., Shariatmadari H. and Mirghaffari N., Modification of rice hull and sawdust sorptive characteristics for remove heavy metals from synthetic solutions and wastewater. J. Hazard. Mater. 154 (2008), 451–458.

[18] Lorenc-Grabowska E., Gryglewicz G.and Diez M.A., Kinetics and equilibrium study of phenol adsorption on nitrogen-enriched activated carbons. Fuel 114 (2013), 235–243.

[19] Chen S., Zhang Sh., Zhou X., Lv X. and Li Y., Low temperature preparation of the Zn_2SiO_4 ceramics with the addition of BaO and B2O3. J. Mater. Sci.- Mater. Electron. 22 (2011),1274–1281.

[20] Romero-Anaya A.J., Molina A., Garcia P., Ruiz-Colorado A. A., Linares-Solano A. and Salinas-Martı´nez de Lecea C., Phosphoric acid activation of recalcitrant biomass originated in ethanol production from banana plants. Biomass Bioenergy 35 (2011), 1196-1204.

[21] Moreno-Barbosa J. J., Lo´pez-Velandia C., Maldonado A. D. P., Giraldo L. and Moreno-Piraja´n J. C., Removal of lead(II) and zinc(II) ions from aqueous solutions by adsorption onto activated carbon synthesized from watermelon shell and walnut shell. Adsorption 19 (2013), 675–685.

[22] de Celis J., Amadeo N. E and Cukierman A. L., In situ modification of activated carbons developed from a native invasive wood on removal of trace toxic metals from wastewater. J. Hazard. Mater. 161 (2009), 217–223.

[23] Cullity B.D., "Elements of X-ray Diffraction", 2nd ed., Addison-Wesley, Reading, MA, (1978) pp. 101-102.

[24] PangiliInan-Ferolin T. and Vequizo R. M., Synthesis of Zinc Silicate Using Silica from Rice Hull Ash (RHA) Through Solid-State Reaction, Proceedings of the IETEC'13 Conference, Ho Chi Minh City, Vietnam. Copyright © Tender Pangilinan-Ferolin and Reynaldo M. Vequizo, 2013.

[25] Takesue M., Hayashi H. and Smith R. L., Thermal and chemical methods for producing zinc silicate (willemite): A review. Prog. Cryst. Growth Charact. Mater. 55 (2009), 98-124.

[26] Galiatsatou P., Metaxas M. and Kasseloui-Rigopoulou V., Mesopores activated carbon from agriculturalby products. Mikrochim. Acta 136 (2001), 147-152.

[27] Sharma, P. and Bhatti, H., Laser induced down conversion optical characterizations of synthesized Zn − $MnxSiO_4$ nanophosphors. J. Alloys Compds. 473 (2009), 483-489.

[28] Roy A., Polarz S., Rabe S., Rellinghaus B., Zähres H. and Kruis F. E. First preparation of nanocrystalline zinc silicate by chemical vapor synthesis using an organometallic single-source precursor. Chem. Eur. J. 10 6 (2004), 1565–75.

[29]Obiora-Okafo I. A. and Onukwuli O. D., Utilization of Sawdust (*Gossweilerodendron balsamiferum)* as an Adsorbent for the Removal of Total Dissolved Solid Particles from Wastewater. I.j.multidiscip.sci.and eng., 4 4 (2013), 45-53.

[30] AlOthman Z. A., Habila M.A.and Ali R. (2011) Preparation of Activated Carbon Using the Copyrolysis of Agricultural and Municipal Solid Wastes at a Low Carbonization Temperature, International Conference on Biology, Environment and Chemistry.72-76.

[31] Pavia D. l, Lampman G. M. and Kaiz G. S. (1987). Introduction to Spectroscopy: A Guide for Students of Organic Chemistry. WB Saunders, Philadelphia.

[32] Wang L., Zhou Y. and Qiu J., Influence of pore structures on the electrochemical performance of asphaltene-based ordered mesoporous carbons. Microporous Mesoporous Mater. 174 (2013), 67–73.

[33] Sing KW, Everet DH, Haul R., Moscou L, Pierotti RA, Rouquero J., Siemieniewasa T (1985) Pure Applied Chem. 57:603–619.

[34] Hassan H. S., Attallah M. F. and Yakout S. M., Sorption characteristics of an economical sorbent material used for removal radioisotopes of cesium and europium. J. Radioanal. Nucl. Chem. 286 (2010), 17–26.

[35] Everett D. H. (1967), Adsorption Hysteresis in The solid-gas interface Volume 2 Edited by E. Alison Flood, Marcel Dekker, Inc., New York, p. 1059-1060.

[36] Linsen B. G. and Heuvel V. D. (1976) Pore Structure in The solid-gas interface Volume 2 Edited by E. Alison Flood, Marcel Dekker, Inc., New York, p. 1030-1031.

[37] Lynch M. E., Ding D., Harris W. M., Lombardo J. J., Nelson G. J., Chiu W. K.S. and Liu M., Flexible multiphysics simulation of porous electrodes: Conformal to 3D reconstructed microstructures, Nano Energy 2 (2013), 105–115.

[38] Kosa S., Al-Zhrani G., Abdel-Salam M., Removal of heavy metals from aqueous solutions by multi-walled carbon nanotubes modified with 8-hydroxyquinoline, Chem. Eng. J. 181–182 (2012), 159–168.

[39] Chao H.-P. and Chang Ch.-Ch., Adsorption of copper (II), cadmium (II), nickel (II) and lead (II) from aqueous solution using biosorbents, Adsorption 18 (2012),395–401.

[40] Moreno-Piraján J. C., Garcia-Cuello V. S. and Giraldo L., The removal and kinetic study of Mn, Fe, Ni and Cu ions from wastewater onto activated carbon from coconut shells, Adsorption 17 (2011), 505–514.

[41] Bohli Th., Villaescusa I. and Ouederni A. M., Comparative Study of Bivalent Cationic Metals Adsorption Pb(II), Cd(II), Ni(II) and Cu(II) on Olive Stones Chemically Activated Carbon. J.Chem.Eng. and Process Tech. 4:4 (2013), 1-7.

[42] Lalhruaitluanga H., Jayaram K., Prasad M. N. V. and Kumar K.K. Lead(II) adsorption from aqueous solutions by raw and activated charcoals of Melocanna baccifera Roxburgh (bamboo)—A comparative study. J. Hazard. Mater. 175 (2010), 311–318.

[43] Kumar P. S. and Gayathri R., Adsorption of Pb^{2+} Ions From Aqueous Solutions Onto Bael Tree Leaf Powder: Isotherms, Kinetics and Thermodynamics Study. J. Eng. Sci.and Tech. 4 4 (2009), 381 – 399.

[44] Nunell G. V., Ferna´ndez M. E., Bonelli P. R. and Cukierman A. L. ,Conversion of biomass from an invasive species into activated carbons for removal of nitrate from wastewater, Biomass Bioenergy 44 (2012), 87-95.

[45] Ciesielczyk F., Bartczak P., Wieszczycka K., Siwin´ska-Stefan´ska K., Nowacka M., Jesionowski T., Adsorption of Ni(II) from model solutions using co-precipitated inorganic oxides. Adsorption 19 (2013), 423–434.

[46] Barany S. and Strelko V., Laws and mechanism of adsorption of cations by different ion-exchange forms of silica gel, Adsorption 19 (2013),769–776.

[47] Gad. H. M. H. and Maziad N. A.,Radiation Copolymerization of Styrene/Acrylic Acid Grafted to Silica Surface For separation and purification purposes:1.Characterization and sorption of some organic compounds and Metals. IJAS TR. 4 4 (2014), 184-201.